Biosensors and Bioelectronics 127 (2019) 50–56

Contents lists available at ScienceDirect

Biosensors and Bioelectronics

journal homepage: www.elsevier.com/locate/bios

Universal method for direct bioconjugation of electrode surfaces by fast enzymatic polymerization

Sumit Kumar[a,1], Al-Monsur Jiaul Haque[b,1], Jonathan Sabaté del Río[a], Shreedhar Gautam[a], Yoon-Kyoung Cho[a,b,*]

[a] Center for Soft and Living Matter, Institute for Basic Science (IBS), Ulsan 44919, Republic of Korea
[b] Department of Biomedical Engineering, School of Life Sciences, Ulsan National Institute of Science and Technology (UNIST), Ulsan 44919, Republic of Korea

ARTICLE INFO

Keywords:
Electrode modification
Bioconjugation
Tannic acid
Enzymatic polymerization

ABSTRACT

We report HRP-catalyzed polymerization of Tannic acid (TA) and application of the poly (Tannic acid) (p(TA)) as a versatile platform for covalent immobilization of biomolecules on various electrode surfaces based on electrochemical oxidation of the p(TA) and subsequent oxidative coupling reactions with the biomolecules. We also used this method for capturing cancer cells through a linker molecule, folic acid (FA). Furthermore, we have demonstrated that enhanced electrocatalytic activity of the p(TA)-modified surface could be used for simultaneous electrochemical determination of biologically important electroactive molecules such as ascorbic acid (AA), dopamine (DA), and uric acid (UA). This HRP-catalyzed polymerization of TA and p(TA)-mediated surface modification method can provide a simple and new framework to construct multifunctional platforms for covalent attachment of biomolecules and development of sensitive electrochemical sensing devices

1. Introduction

Surface modification of electrodes to generate a desired functionality or a specific property is often the primary step in developing devices for various applications such as sensing, catalysis, and energy storage (Willner, 2002; Mattiuzzi et al., 2012; Wang et al., 2015; Labib et al., 2016; Perez-Mitta et al., 2017). Commonly used methods for electrode surface modification, (*e.g.*, a self-assembled monolayer (SAM) of alkane thiols, silanization of organosilanes, and azide-alkyne based click chemistry) suffer from various limitations such as finite substrate materials, long incubation times, poor stability, and multistep procedures. Thus, considerable efforts have been expended in recent years to develop a simple, rapid, biocompatible, and versatile method to modify different electrode surfaces (Janissen et al., 2017; Cao et al., 2017).

Inspired by the bioadhesive property of marine mussels, phenolic-based coatings have been developed as a substrate-independent strategy for multifunctional surface engineering (Lee et al., 2007; Sileika et al., 2013). Recently, tannic acid (TA) has become attractive for coatings because of the large number of hydroxyl groups and multiple aromatic rings that allow for hydrogen and ionic bonding as well as hydrophobic interactions with a variety of material surfaces (Sileika et al., 2013; Ejima et al., 2013; Fan et al., 2017a; Fan et al., 2017b; Xu et al., 2017). TA has been used as a gelation binder, coating membrane separator, in layer-by-layer film formation, supramolecular hydrogel formation, modification of inorganic and polymeric nanoparticles, and antibiofouling and antibacterial activity (Fan et al., 2017a; Fan et al., 2017b; Xu et al., 2017; Hegab et al., 2016; Abouelmagd et al., 2016; Shin et al., 2015; Rajar et al., 2017; Fan et al., 2017a; Fan et al., 2017b; Pan et al., 2015; Fang et al., 2017; Xu et al., 2016; Jiao et al., 2014; Hu et al., 2017). However, spontaneous self-polymerization of TA is a very slow process for which a long incubation time is required. The further functionalization of TA is also technically challenging and inefficient because of the limited number of reactive quinone groups present. Therefore, a simple method involving faster polymerization of TA and quick activation for generating more reactive quinone groups is desired for constructing a multifunctional platform.

Enzyme-catalyzed polymerization is of much interest in polymer synthesis as it can provide various functional polymers with higher rates and greater specificity under mild conditions that are difficult to obtain using conventional chemical catalysts. Peroxidase is well known for inducing the oxidative polymerization of phenolic compounds under mild reaction conditions (Kawakita et al., 2009). Electrochemical activation of hydroquinone or catechol-terminated self-assembled monolayers to their corresponding quinone forms has been used as a rapid

* Corresponding author at: Center for Soft and Living Matter, Institute for Basic Science (IBS), Ulsan 44919, Republic of Korea.
E-mail address: ykcho@unist.ac.kr (Y.-K. Cho).
[1] These authors contributed equally.

https://doi.org/10.1016/j.bios.2018.12.017
Received 23 September 2018; Received in revised form 23 November 2018; Accepted 10 December 2018
Available online 13 December 2018
0956-5663/

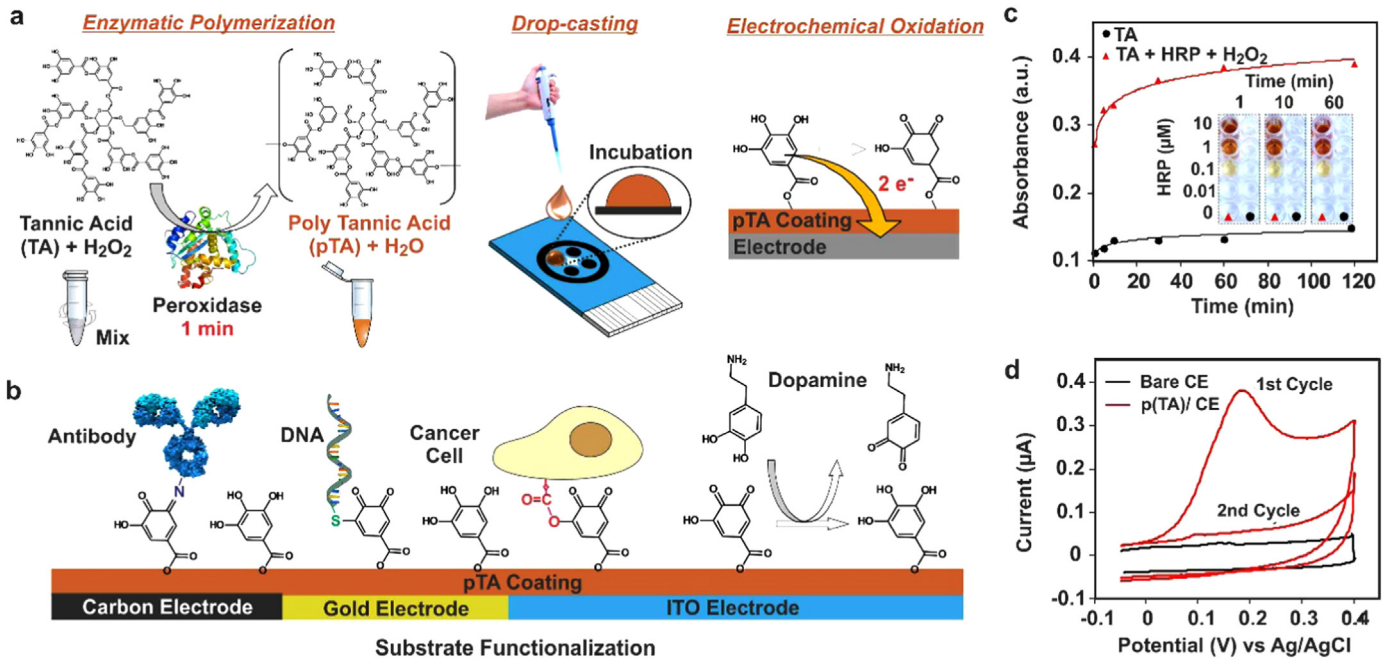

Fig. 1. Electrochemical oxidation of horseradish peroxidase (HRP)-accelerated polymerization of tannic acid and its versatile applicability in direct bioconjugation. (a) Tannic acid (colorless) polymerization increased ~500-fold under HRP catalysis (with H_2O_2 as the oxidant) (dark brown) and it was further electrochemically activated for surface functionalization. (b) Schematic of surface modification of a variety of electrode surfaces. A versatile technology for covalent conjugation of biomolecules with a variety of functional groups on the electrode surface. (c) Visual observation and UV–visible absorbance at 356 nm of TA polymerization at various time points with and without HRP. (d) Cyclic voltammograms of bare and p(TA)-coated carbon electrode (CE) surfaces to determine the oxidation peak current.

and reagentless process for covalent coupling of small molecules, larger proteins, or nucleic acids (Furst et al., 2017; Kwon and Mrksich, 2002; Yousaf and Mrksich, 1999; Kim et al., 2004). Based on the above observations, we reasoned that horseradish peroxidase (HRP) can catalyze the polymerization of TA and that electrochemical activation of the polymer can be very effective to generate more quinone groups for efficient covalent conjugation of (bio)molecules.

Herein, a new method based on enzyme accelerated polymerization of TA has been described that allows efficient coupling of different biomolecules on material-independent electrode surfaces by generating a thin layer of poly(tannic acid) (p(TA)) within minutes (Fig. 1**a**). HRP-catalyzed polymerization of TA produced p(TA), which was then coated on nonmetal, metal, and metal oxide electrode surfaces. Further, the p(TA)-coated surface was utilized as a multifunctional platform for conjugation of receptor biomolecules or small molecules, and the electrocatalytic detection of biologically relevant electroactive small molecules (Fig. 1**b**).

This method was also used for patterning multiple receptor molecules on the specific electrode surfaces on the same sensor chip. Covalent conjugation of the molecules was based on electrochemical oxidation of p(TA) and subsequent oxidative coupling of the biomolecules through Michael-type addition/Schiff base reaction. As a proof of concept, this versatile method was utilized for the immobilization of an antibody and subsequent detection of interleukin-6 (IL-6), a single-stranded DNA sequence, and the linker molecule, folic acid (FA) for the selective capturing of cancer cells. The enhanced electrocatalytic activity of the p(TA)-modified surface was used for the simultaneous detection of biologically relevant electroactive molecules such as ascorbic acid (AA), dopamine (DA), and uric acid (UA).

2. Experimental section

2.1. Materials and chemicals

Tannic acid, HRP, hydrogen peroxide (H_2O_2), folic acid, dopamine hydrochloride, uric acid, ascorbic acid, and hexaammineruthenium(III) chloride were purchased from Sigma-Aldrich. Tris-HCl (1.5 M, pH 8.8) was purchased from Biosesang Inc. Alexa Fluor (488)-labeled goat anti-rabbit IgG and PE-labeled goat anti-mouse IgG were purchased from Bio Reagents. IL-6 Human Matched Antibody Pair (containing IL-6 antigen, IL-6 capture antibody, biotinylated IL-6 detection antibody, and HRP conjugated streptavidin) was purchased from Invitrogen. Single-stranded DNA was purchased from Integrated DNA Technologies. Unless otherwise stated, all reagent-grade chemicals were used as received and 18.2 MΩ cm ultrapure deionized water was used to prepare all buffer and aqueous solutions. 3,3′,5,5′-Tetramethylbenzidine (TMB) substrate that precipitates upon reaction with HRP was purchased from Sigma-Aldrich (TMB Enhanced One Component HRP Membrane Substrate). Screen-printed carbon electrodes were purchased from Korea Total Printing Technology. Indium tin oxide (ITO)-coated glass slides and gold rod electrodes (2 mm diameter) were purchased from Sigma-Aldrich and Qrins, respectively.

2.2. Preparation of p(TA) solution

First, small amounts of stock solutions of TA (3 mg/mL), H_2O_2 (1 M), and HRP (10 μM) were prepared in Tris-HCl buffer (10 mM, pH 8.5). Next, a 100 μL 2 mg/mL p(TA) solution was prepared by mixing 66.6 μL TA, 21.4 μL Tris-HCl buffer, 2 μL H_2O_2, and 10 μL HRP solutions, followed by vortex mixing for a short while. The p(TA) solution was freshly prepared and used.

2.3. Preparation of p(TA)-coated electrode surfaces

Screen-printed carbon electrodes on plastic were used without any pretreatment. ITO and gold electrodes were first washed with ethanol and water and then dried under a stream of N_2 gas. The electrodes were treated with piranha solution for several minutes, followed by washing with copious amounts of water and drying under a stream of N_2 gas. A drop of the freshly prepared p(TA) solution was applied on the cleaned

electrode surfaces and incubated for 30 min in a humid chamber, followed by washing with Tris-HCl buffer and water, and drying under a stream of N_2 gas.

2.4. Immobilization of the antibody on the p(TA)-coated electrode surface

The p(TA)-coated electrode surfaces were electrochemically oxidized either by carrying out a potential cycle from 0.0 to 0.4 V or applying a potential of 0.3 V for 20 s. After washing with water and drying with N_2 gas, the oxidized electrodes were incubated with a drop of the fluorescence group-labeled antibody solution (20 μg/mL in PBS) for 2 h at room temperature in a humid chamber. The electrodes were then washed with PBS and water and dried under a stream of N_2 gas. Finally, immobilization of the antibody was confirmed by fluorescence microscopy images of the modified electrodes.

2.5. Attachment of cancer cells on the p(TA)-coated electrode surface

As described above, the p(TA)-coated electrode surfaces were electrochemically oxidized and treated with folic acid (FA) solution for 2 h, followed by washing with water and drying with N_2 gas. Then, the electrodes were incubated with a drop of MCF-7 cell solution for 2 h, followed by washing with water and drying with N_2 gas. Finally, the attachment of the cells on the FA-conjugated electrode surfaces was confirmed by fluorescence microscopy and scanning electron microscopy (SEM) images of the modified electrodes.

2.6. Immobilization of the DNA on the p(TA)-coated electrode surface

As described above, the p(TA)-coated electrode surfaces were electrochemically oxidized and incubated with a drop of thiolated single-stranded DNA (HS-$(CH_2)_6$-AAAGGAAAGGGAAAGGGAAGGGAAG-FL) solution for 2 h at room temperature in a humid chamber. Subsequently, the electrodes were washed with PBS and water and dried under a stream of N_2 gas. Cyclic voltammetry (CV) was carried out in PBS buffer solution containing 50 μM $[Ru(NH_3)_6]^{3+}$ after 1 min incubation.

2.7. Electrochemical measurements

Electrochemical measurements were carried out with a three-electrode system consisting of a p(TA)-coated electrode, Ag/AgCl electrode, and Pt wire as the working, reference, and counter electrodes, respectively, in Tris-HCl buffer (pH 8.5) with a scan rate of 50 mV/s. In the case of the carbon electrode surface, Ag/AgCl paste and a screen-printed carbon electrode were used as the pseudo-reference and counter electrodes, respectively.

2.8. Electrochemical detection of IL-6

The p(TA)-coated CE electrode surfaces were electrochemically oxidized in PBS by square wave voltammetry (SWV), carrying out a sweep from 0.0 to 0.7 V with a pulse height of 30 mV, pulse width of 100 ms, and step height of 1 mV. After drying with N_2 gas, the oxidized electrodes were incubated with a 5 μL drop of IL-6 capture antibody solution (125 μg/mL in PBS) overnight at 4 °C in a water saturated chamber. Next, the electrode chips were immersed in a Petri dish with washing buffer (PBS containing 0.05% Tween 20) under shaking for 10 min, to remove non-specific adsorbed IL-6 capture antibodies, and dried under a gentle stream of N_2 gas. The electrode chips were then submerged in a Petri dish with assay buffer (PBS containing 0.05% Tween 20% and 0.01% BSA) for 30 min to block non-specific sites. Then, a sandwich ELISA was carried out on each electrode by preparing all the reagents in the assay buffer, incubating each step with 5 μL volume per electrode, and washing with the buffer after each step. First, IL-6 was incubated at different concentrations for 1.5 h, a secondary antibody (1 μg/mL) for 1 h, and HRP-conjugated streptavidin (5 μg/mL) for 30 min. Finally, the TMB Substrate was incubated on the electrodes for 1 min, this is a specific formulation of ELISA substrate that precipitates upon oxidation with HRP, and therefore typical diffusion of reacted TMB to nearby electrodes yielding non-specific signal output is eliminated. After a minute, the substrate was washed with PBS, and the remaining precipitated substrate on the electrodes containing TMB was measured by SWV using the same conditions as those used for the oxidation of p(TA), measuring the current height of subsequent TMB oxidation. A calibration curve was built by plotting the current height obtained for each concentration of IL-6.

2.9. Instruments and characterizations

UV–visible absorbance spectra were obtained with a Tecan Infinite M200 PRO reader using a NanoQuant plate. Attenuated total reflectance Fourier-transform infrared (ATR-FTIR) spectra were obtained with an ATR-FTIR spectrophotometer (Varian). X-ray photoelectron spectroscopy (XPS) was performed with an XPS system (ThermoFisher, K-alpha). SEM images were obtained using a cold field-emission scanning electron microscope (Hitachi High-Technologies, S-4800) at 10 kV. An Olympus IX-71 inverted fluorescence microscope equipped with a CCD camera was used for fluorescence images. MetaMorph and ImageJ image analysis software were used to identify the regions of interest and process the images of the modified electrodes. Water contact angle measurements were carried out with a digital contact angle goniometer (Ramé-hart instrument co.) using a 5 μL drop of deionized water on the bare and modified electrode surfaces.

3. Results and discussion

3.1. Characterization of TA polymerization and coating of the p(TA) on electrode surfaces

As shown in Fig. 1**c** (and Fig. S1), the colorless TA solution turned brown within one minute in the presence of HRP and H_2O_2, whereas it remained colorless even after several hours in the absence of HRP. In addition, the amount of color change was dependent on the concentrations of HRP, indicating that HRP catalyzed the polymerization of TA. In UV–visible spectroscopy, the absorption maximum of the TA solution was blue-shifted and a new peak was observed at a higher wavelength (~356 nm) corresponding to the formation of quinone groups, which was attributed to the oxidative polymerization of TA (Fig. S2). Indeed, it is well known that peroxidase action on phenolic compounds leads to the formation of quinones and induces a quinone-based coupling process in the phenolic compounds (Kawakita et al., 2009). The absorbance at 356 nm of the TA solution containing HRP and H_2O_2 reached, within 1 min, a higher value than that of TA solution alone even after several hours (Fig. 1**c**).

A screen-printed carbon electrode (CE) was coated with p(TA) by incubation in the polymer solution for 30 min. Subsequently, CV measurements were performed on the coated surface in Tris-HCl buffer solution. A clear oxidation peak of 0.38 μA at 0.2 V was observed during the first cycle, which diminished in intensity in the subsequent cycles, as already observed in previous studies (Wan et al., 2007; Maerten et al., 2017), indicating a complete and irreversible oxidation of the p(TA) layer on the CE surface during the first cycle (Fig. 1**d**). The oxidation peak current did not increase on prolonging the incubation time over 30 min, which indicated a saturated coating of the electrode surface by that time (Fig. S3). In ATR-FTIR measurements, the broad peak at 3000 cm^{-1} was ascribed to the –OH stretching vibration on the TA-coated surface, which weakened in intensity after oxidation. Other peaks at 1027 cm^{-1} (C-O-C bending mode) and 1660 cm^{-1} (stretching vibration of C=O) were stronger after oxidation (Fig. 2**a**). The p(TA) coating on the CE surface and electrochemical oxidation of p(TA) were further confirmed by XPS measurements. As shown in Fig. 2**b** (and Fig.

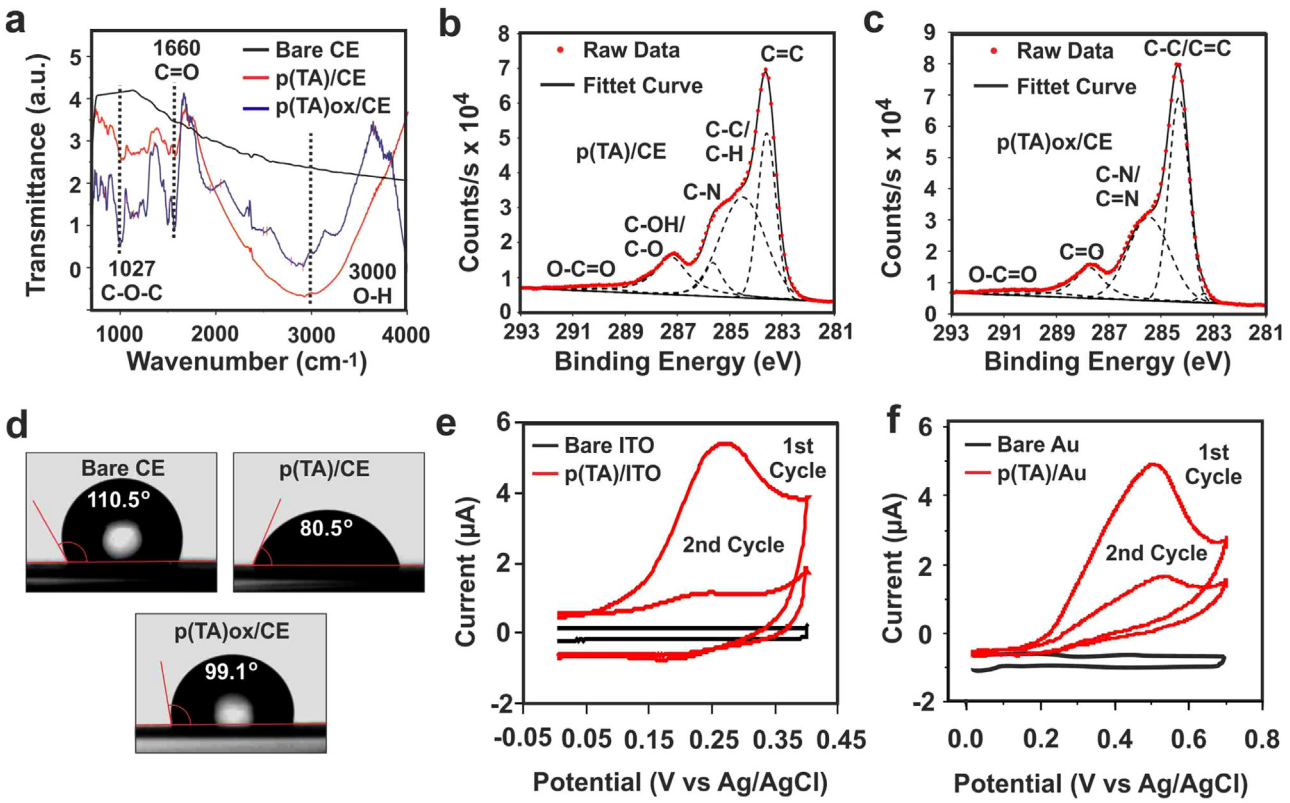

Fig. 2. Characterization of electrochemically oxidized p(TA) surfaces. (a) ATR-FTIR spectra of bare, p(TA) and $p(TA)_{ox}$ on the carbon electrode surface. (b) XPS spectra of the p(TA) coated carbon electrode. (c) XPS spectra of electrochemically oxidized p(TA) coated carbon electrode surfaces. (d) Water contact angle measurements of bare, p(TA) and $p(TA)_{OX}$ coated carbon electrode surfaces. (e) Cyclic voltammograms of p(TA)-coated ITO. (f) Cyclic voltammograms of p(TA)-coated Au electrode surfaces in Tris-HCl buffer at a scan rate of 50 mV/s.

S4), the peak intensities at binding energies corresponding to different oxygen-containing functional groups in C 1s spectra, and primary amine/peptide bonds in N 1s spectra, were higher on the p(TA)-coated CE surface as compared to the bare CE surface, indicating the presence of p(TA)-containing HRP. The C 1s peaks at 283.5 eV and 287 eV on the p(TA)-coated CE surface were slightly shifted to 284.3 eV and 288 eV after electrochemical oxidation, which was likely due to the conversion of C=C to C-C and C-O/OH to C=O (Fig. 2**c**).

The surface properties of the p(TA)-coated CE were also examined by measuring the water contact angles before and after electrochemical oxidation and comparing these to the bare surface. As shown in Fig. 2**d**, the contact angle decreased from 110.5 ± 0.05° to 80.5 ± 0.1° for the p(TA)-coated surface. This indicates that the surface became more hydrophilic after coating with p(TA) because of the presence of a large number of –OH groups. The contact angle increased again to 99.1 ± 0.1° after electrochemical oxidation, resulting in reduced hydrophilicity. Combined results from the CV, ATR-FTIR, XPS, and water contact angle measurements indicate the successful coating and subsequent electrochemical oxidation of p(TA) on the CE surface. The coating of p(TA) on ITO and gold electrode surfaces was also confirmed by CV (Figs. 2**e,** 2**f**) and XPS (Fig. S4). A clear oxidation peak was observed at 0.25 V and 0.5 V for ITO and gold electrode respectively during the first cycle, which was largely decreased in intensity in the 2nd cycle indicating an irreversible oxidation of the p(TA) during the first cycle. Though it is noted that the 2nd cycle of CV for pTA on ITO is more reversible, which is not on the Au, we can hardly see a reduction process for the ITO either, and therefore we believe it is not significant. Though we are not sure about the exact reasons behind this difference, it can be due to the difference in surface topography of pTA on two electrodes

The surface coverage (Γ) of p(TA) on the CE was calculated with the equation $\Gamma = Q/nFA$, where $Q = 2 \times 10^{-6}$ C and is the electric charge obtained by integrating the area under the anodic peak with a background correction. n = 1 and is the number of electrons transferred for the oxidation reaction. F = 96,485 C/mol and is the Faraday constant, and A = 0.067 cm^2 and is the effective surface area of the electrode. The calculated surface coverage, 3.05×10^{-10} mol/cm^2, is 10-fold lower than a reported value for free TA deposited on a glassy carbon electrode modified with single walled carbon nanotubes (SWCNTs/GC) (Wan et al., 2007). This phenomenon is attributed to the different electrode functionalization and the TA oxidation method. Wan *et al.* used SWCNTs/GC, which is known to increase the active surface area of the electrode allowing a larger amount of TA to be deposited, thus yielding a larger charge and therefore a larger value of surface coverage compared to the value we obtained using the bare CE. Furthermore, Wan et al. measured the charge from a direct electrochemical oxidation of a concentrated solution of TA (15 μM) onto the electrode surface, thus fresh TA could diffuse from the bulk solution towards the surface of the electrode. In our work, we first drop-casted p(TA) on the electrode, then washed the surface, and finally electrochemically oxidized the attached p(TA). With this method we are certain that the oxidation charge measured comes only from p(TA) attached to the surface of the electrode and not from fresh TA molecules diffusing towards the electrode.

3.2. Conjugation of receptor biomolecules or small molecules on the p(TA)-coated surfaces

Under oxidizing conditions, a catechol-rich surface can support covalent coupling reactions with nucleophiles such as amine or thiol-containing molecules via a Michael-type addition or Schiff base reaction to create multifunctional platforms (Fig. 3**a**). Such electrode

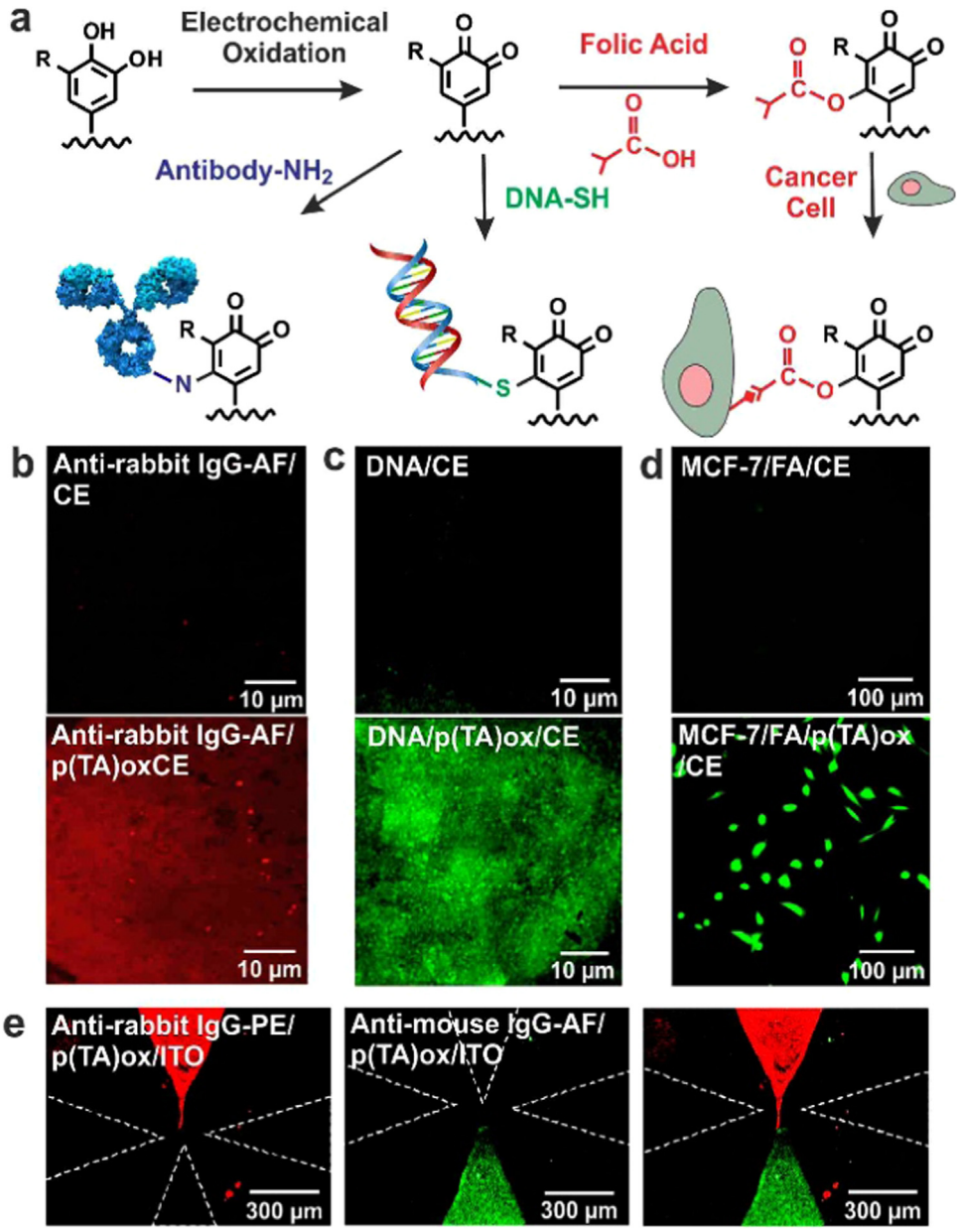

Fig. 3. Surface functionalization of the electrode. (a) Strategy for conjugation of biomolecules with different functional groups on the electrode surface. (b) Fluorescence images for covalent conjugation of fluorophore labeled antibodies with and without $p(TA)_{ox}$ on the electrode surface. (c) Fluorescence images for covalent conjugation of thiolated DNA with and without $p(TA)_{ox}$ on the electrode surface. (d) Fluorescence images for the selective capture of cancer cells with and without $p(TA)_{ox}$ on the electrode surface. (e) Covalent conjugation of different fluorophore labeled antibodies on the same electrode array surface.

surface can be applicable to generate either a single analyte sensing platform by immobilizing an amine or thiol terminated capture probe (*e.g.* antibody or DNA) on a plane electrode surface, or multiplex biosensor platforms by selective electrochemical activation of the electrodes of interest and sequential immobilization of multiple capture probes on an electrode array. Therefore, the conjugation of a fluorophore-labeled antibody (Alexa fluor® 568-labeled anti rabbit IgG) on p(TA)ox/CE was examined by strong red fluorescence on the p(TA)ox electrode surface, indicating efficient conjugation, with only a few scattered weak fluorescence spots observed for the bare CE surface (Fig. 3**b**). The conjugation of thiol-terminated single-stranded SH-DNA-Fluorescein on a p(TA)ox/CE surface was also studied by strong green fluorescence (Fig. 3**c**). Furthermore, CV of a 50 μM $Ru(NH_3)_6Cl_3$ solution before and after incubating the modified surfaces with the DNA solution was also performed. As shown in Fig. 4, a higher redox peak current was observed for the DNA/p(TA)ox/CE surface, which indicated the conjugation of the DNA strand on the surface because of the accumulation of positively charged $[Ru(NH_3)_6]^{3+}$ on the negatively charged phosphate backbone of the DNA through electrostatic attraction.

A major challenge to the study of the many types of cells is their lack of binding to surfaces. To capture cancer cells, the p(TA)ox/CE surface was functionalized with folic acid (FA) and incubated with a solution of MCF-7 cells (breast cancer cell line) and MCF-10A (breast normal cell line). The surface was washed after 30 min and the selective capture of cancer cells was examined by fluorescence microscopy and SEM (Fig. 3**d** and Fig. S5). As shown in the Fig. S6, after modification of FA to p(TA)ox/CE the results indicated the selective binding of cancer cells comparable to normal cells.

Additional experiments were carried out in order to investigate the possibility of spatial control of the p(TA) coating for bioconjugation, as well as the conjugation of multiple receptor molecules on the same

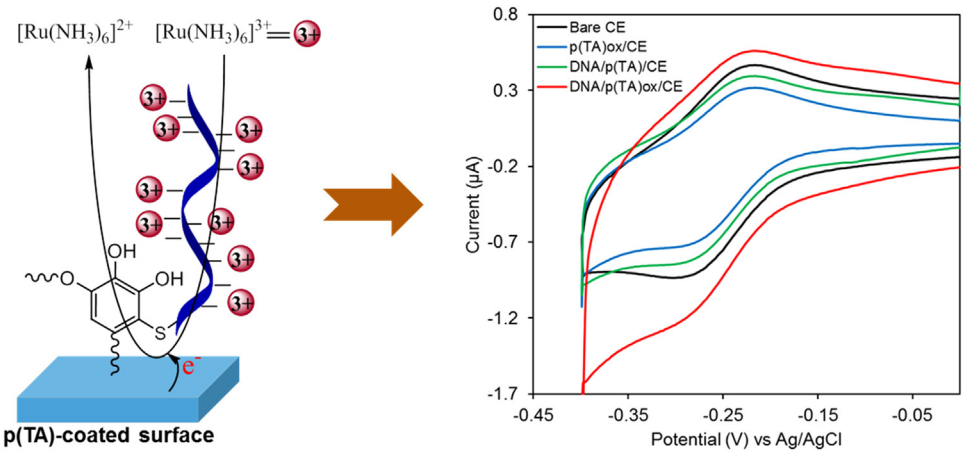

Fig. 4. Schematic representation of electrochemical reduction of positively charged ruthenium complex electrostatically attached to the negatively charged backbone of DNA strand immobilized on the p(TA)ox-modified surface, and cyclic voltammograms obtained at bare and modified carbon electrode (CE) surfaces in 10 mM Tris-HCl buffer (pH 7.6) containing 50 μM $[Ru(NH_3)_6]^{3+}$ at a scan rate of 50 mV/s after 1 min incubation. The reduction current of the cyclic voltammogram obtained at the DNA and p(TA)ox-modified surface was higher compared to that at other surfaces, indicating the successful immobilization of DNA on the p(TA)ox-coated electrode surface.

electrode surface. An ITO electrode surface was covered with a mask and incubated with a p(TA) solution for the selective formation of a p(TA) layer on the exposed area. The modified surface was then electrochemically oxidized and incubated with a solution of a fluorophore labeled antibody. As shown in Fig. 3**e**, red fluorescence was observed only on the p(TA)-coated area of the electrodes. Likewise, different antibodies could be immobilized in close proximity on the same ITO electrode surface (Fig. 3**e**).

3.3. Sandwich ELISA on a p(TA)-coated electrode surface

To verify the viability of the p(TA)-coated electrodes for biosensing, the p(TA)ox/CE electrodes were functionalized with anti-IL-6 capture antibodies and a sandwich ELISA was performed. First, different concentrations of the antigen IL-6 were incubated on each electrode, followed by a biotinylated detection antibody, and finally the HRP-conjugated streptavidin. Following the addition of TMB Substrate, the concentration of IL-6 was measured electrochemically by SWV, and the current height of the subsequent oxidation of the precipitate was used as readout signal to build an IL-6 calibration curve, yielding a linear range between 7.8 and 125 pg/mL, a limit of detection of 8.1 pg/mL and a sensitivity of 0.89 μA mL/pg (Fig. 5**a**). The effect of remaining HRP present in the p(TA)-modified CE was first evaluated visually by incubating the p(TA)-modified CE in ELISA substrate for up to 30 min, but no color change was observed. Furthermore, after this incubation with TMB, the electrodes were electrochemically monitored by SWV to check the presence of oxidized TMB. Signal outputs below 20 μA were obtained, comparable to the blank signal outputs shown in the calibration curve of IL-6. Thus, we think that this signal output is due to non-specific adsorption of the ELISA substrate on the p(TA)-modified CE rather that a reaction with the remaining HRP entrapped in the p(TA).

3.4. Simultaneous detection of electroactive small molecules using a p(TA)-coated surface

Additionally, the electrocatalytic activity of the p(TA)-coated electrode surface towards several physiologically relevant electroactive small molecules such as ascorbic acid (AA), dopamine (DA), and uric acid (UA) was examined. As shown in Fig. S7, the oxidation peak currents for all three molecules were higher on the p(TA)-coated electrode surfaces as compared to the bare electrode. These results clearly illustrate a higher electrocatalytic activity of the p(TA)-coated surface as compared to that of the bare surface, which suggests a faster heterogeneous electron transfer through the p(TA) layer given that it consists of π-electron-rich aromatic groups. SWV with a solution containing AA, DA, and UA at the bare and p(TA)-coated surfaces was also performed for assessing the possibility of simultaneous detection of the molecules. Three individual oxidation peaks corresponding to AA, DA and UA were clearly observed in the voltammogram from the p(TA)-coated surface (Fig. 5**b**), whereas only two peaks with lower currents were observed in the voltammogram from the bare surface. This result suggested that the p(TA)-coated surface could potentially be used for the simultaneous electrochemical detection of different electroactive molecules. The sensitivity, linear range and LOD was determined from the calibration curve for each analyte separately (AA, DA and UA) by measuring the oxidation peak height in SWV at different concentrations (Fig. S8). The peak currents exhibited a linear relationship with the concentrations of AA, DA, and UA in the ranges of 7–100, 2–15, and 2–250 μmol/l, with detection limits of 0.2, 0.3, and 0.4 μM, respectively. These results are similar to a previously reported work using hemin functionalized graphene oxide modified glassy carbon electrodes (Zou et al., 2007).

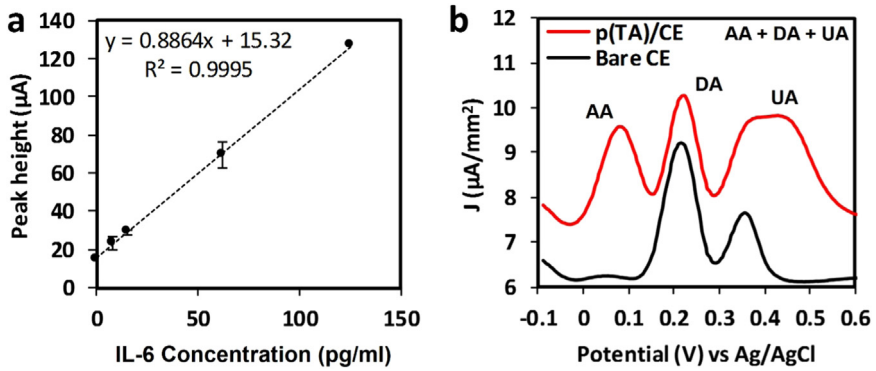

Fig. 5. Biosensing application of p(TA)-modified CE electrodes. (a) Calibration curve of IL-6 concentration between 7.8 and 125 pg/mL. (b) Square wave voltammograms obtained at the bare and $p(TA)_{ox}$-modified carbon electrodes in 10 mM PBS (pH 7.4) containing 100 μM AA + 100 μM DA + 200 μM UA.

4. Conclusion

In conclusion, a new method has been developed for the fast polymerization of TA and its rapid coating on nonmetal, metal, and metal oxide electrode surfaces. It was shown that the p(TA)-coated electrode surface could be used as a multifunctional platform for the covalent conjugation of biomolecules and small molecules, and to pattern biomolecules at specific locations as well as multiple receptor molecules on the different electrode surfaces on the same sensor chip. In addition, the enhanced electrocatalytic activity of p(TA) was exploited for the simultaneous electrochemical detection of several biologically relevant electroactive molecules. This enzyme-enhanced polymerization and electrochemical surface activation and functionalization method is a simple, fast, and versatile framework to construct multifunctional platforms on different electrode surfaces for the development of multiplex electrochemical biosensors.

Acknowledgments

This work was supported by the taxpayers of South Korea through the Institute of Basic Science (IBS-R020-D1).

Supporting information

Additional data and characterization (PDF).

Notes

The authors declare no competing financial interests.

Declaration of interests

None.

Appendix A. Supplementary material

Supplementary data associated with this article can be found in the online version at https://doi.org/10.1016/j.bios.2018.12.017.

References

Abouelmagd, S.A., Meng, F., Kim, B.-K., Hyun, H., Yeo, Y., 2016. ACS Biomater. Sci. Eng. 2, 2294.
Cao, C., Zhang, Y., Jiang, C., Qi, M., Liu, G., 2017. ACS Appl. Mater. Interfaces 9, 5031.
Ejima, H., Richardson, J.J., Liang, K., Best, J.P., van Koeverden, M.P., Such, G.K., Cui, J., Caruso, F., 2013. Science 341, 154.
Fang, Y., Gonuguntla, S., Soh, S., 2017. ACS Appl. Mater. Interfaces 9, 32220.
Fan, H., Wang, J., Zhang, Q., Jin, Z., 2017a. ACS Omega 2, 6668.
Fan, H., Wang, L., Feng, X., Bu, Y., Wu, D., Jin, Z., 2017b. Macromolecules 50, 666.
Furst, A.L., Smith, M.J., Francis, M.B., 2017. J. Am. Chem. Soc. 139, 12610.
Hegab, H.M., ElMekawy, A., Barclay, T.G., Michelmore, A., Zou, L., Saint, C.P., Ginic-Markovic, M., 2016. ACS Appl. Mater. Interfaces 8, 17519.
Hu, Z., Berry, R.M., Pelton, R., Cranston, E.D., 2017. ACS Sustain. Chem. Eng. 5, 5018.
Janissen, R., Sahoo, P.K., Santos, C.A., Da Silva, A.M., Zuben, A.A.G.V., Souto, D.E.P., Costa, A.D.T., Celedon, P., Zanchin, N.I.T., Almeida, D.B., Oliveira, D.S., Kubota, L.T., Cesar, C.L., Souza, A.P.D., Cotta, M.A., 2017. Nano Lett. 17, 5938.
Jiao, S., Jin, J., Wang, L., 2014. Talanta 122, 140.
Kawakita, H., Hamamoto, K., Ohto, K., Inoue, K., 2009. Ind. Eng. Chem. Res. 48, 4440.
Kim, K., Jang, M., Yang, H., Kim, E., Kim, Y.T., Kwak, J., 2004. Langmuir 20, 3821.
Kwon, Y., Mrksich, M., 2002. J. Am. Chem. Soc. 124, 806.
Labib, M., Sargent, E.H., Kelley, S.O., 2016. Chem. Rev. 116, 9001.
Lee, H., Dellatore, S.M., Miller, W.M., Messersmith, P.B., 2007. Science 318, 426.
Maerten, C., Lopez, L., Lupattelli, P., Rydzek, G., Pronkin, S., Schaaf, P., Jierry, L., Boulmedais, F., 2017. Chem. Mater. 29, 9668.
Mattiuzzi, A., Jabin, I., Mangeney, C., Roux, C., Reinaud, O., Santos, J., Bergamini, J.-F., Hapiot, P., Lagrost, C., 2012. Nat. Commun. 3, 1130.
Pan, L., Wang, H., Wu, C., Liao, C., Li, L., 2015. ACS Appl. Mater. Interfaces 7, 16003.
Perez-Mitta, G., Tuninetti, J.S., Knoll, W., Trautmann, C., Toimil-Molares, M.E., Azzaroni, O., 2017. J. Am. Chem. Soc. 139, 12610.
Rajar, K., Soomro, R.A., Ibupoto, Z.H., Sirajuddin, Balouch, A., 2017. Int. J. Food Prop. 20, 1359.
Shin, M., Ryu, J.H., Park, J.P., Kim, K., Yang, J.W., Lee, H., 2015. Adv. Funct. Mater. 25, 1270.
Sileika, T.S., Barrett, D.G., Zhang, R., Lau, K.H.A., Messersmith, P.B., 2013. Angew. Chem. Int. Ed. 52, 10766.
Wang, K.-X., Li, X.-H., Chen, J.-S., 2015. Adv. Mater. 27, 527.
Wan, H., Zou, Q., Yan, R., Zhao, F., Zeng, B., 2007. Microchim. Acta 159, 109.
Willner, I., 2002. Science 298, 2407.
Xu, L.Q., Pranantyo, D., Neoh, K.-G., Kang, E.-T., Fu, G.D., 2016. ACS Sustain. Chem. Eng. 4, 4264.
Xu, Z., Wang, X., Liu, X., Cui, Z., Yang, X., Yeung, K.W.K., Chung, J.C., Chu, P.K., Wu, S., 2017. ACS Appl. Mater. Interfaces 9, 39657.
Yousaf, M.N., Mrksich, M., 1999. J. Am. Chem. Soc. 121, 4286.
Zou, H.L., Li, B.L., Luo, H.Q., Li, N.B., 2007. Sens. Actuators B-Chem. 207, 535.